DOI: 10.1002/ejic.201000954

Syntheses, Characterization and Properties of Open-Chain Copper(I) Complexes

Diana Utz,[a,b] Sandra Kisslinger,[a] Frank W. Heinemann,[b] Frank Hampel,[c] and Siegfried Schindler*[a]

Dedicated to Professor Jürgen Heck on the occasion of his 60th birthday

Keywords: Copper / Macrocycles / Oxidation / Oxygen / Helical structures / Anion effect

The coordination chemistry of copper complexes with the ligand **L¹** [**L¹** = {7*E*}-N^1-benzylidene-N^2-{(*E*)-2-(benzylideneamino)ethyl}ethane-1,2-diamine] has been investigated. For copper(I) complexes of **L¹**, the counterion determines the molecular structure in the solid state. The reaction of $[Cu(CH_3CN)_4]PF_6$ with **L¹** yielded the mononuclear complex $[Cu(\mathbf{L^1})(CH_3CN)]PF_6$ (**1**), whereas dinuclear helical $[Cu_2(\mathbf{L^1})_2](ClO_4)_2$ (**2**) resulted from a similar reaction with $[Cu(CH_3CN)_4]ClO_4$. Both compounds have been structurally characterized, and their solution behaviour investigated. Structurally characterized $[Cu(\mathbf{L^1})(PPh_3)]ClO_4$ (**3**) has been synthesized by reacting **2** with PPh_3. Exposure of a solution of **1** towards dioxygen in CH_3OH and CH_2Cl_2 yielded the dinuclear complexes $[Cu_2(\mathbf{L^1})_2(OCH_3)_2](PF_6)_2$ (**4**) and $[Cu_2(\mathbf{L^1})_2(OH)_2](PF_6)_2$ (**5**), respectively. Both compounds have been fully characterized. During the oxidation reaction, no hydroxylation of **L¹** occurred. The oxidation reaction of **1** has been studied by a chemical approach and by UV/Vis spectroscopy, indicating the formation of a peroxido-bridged species during the reaction. Furthermore, by reduction of the imine groups in **L¹** the ligand **L²** [**L²** = N^1-benzyl-N^2-{2-(benzylamino)ethyl}ethane-1,2-diamine] was obtained and the dinuclear copper(II) complex $[Cu_2(\mathbf{L^2})_2Cl_3]PF_6 \cdot 2MeOH$ (**6**) has been structurally characterized.

Introduction

Macrocycles are a special class of ligands that are important for many applications, especially due to their ability to strongly bind metal cations that fit the macrocyclic cavity. Early work from Nelson and coworkers, and followed up by Fenton and coworkers, has shown the versatility of using dialdehydes together with amines to form an interesting group of macrocyclic ligands.[1] Martell and coworkers successfully showed the application of one of these systems to model the reactivity of the copper enzyme tyrosinase. Tyrosinases are monooxygenases that are responsible for the hydroxylation of the phenol residue in tyrosine – forming a catechol – and subsequent two-electron oxidation to the corresponding *o*-quinones.[2] For a better understanding of tyrosinase reactivity, low molecular weight copper complexes have been synthesized as model compounds for this enzyme and their reactivity towards dioxygen has been investigated (only a selected number of examples are reported in the references).[3] The model compound for tyrosinase containing a macrocyclic ligand used by Martell and coworkers was the dinuclear $[Cu_2(mac)(CH_3CN)_2](ClO_4)_2$, where mac is 3,6,9,17,20,23-hexaazatricyclo[23.3.1.1]triaconta-1(29),2,9,11(30),12(13),14,16,23,25,27-decaene (shown in Figure 1), which shows hydroxylation of the aromatic moiety of the ligand upon oxidation.[4]

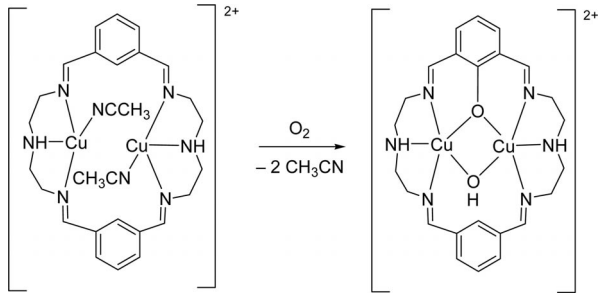

Figure 1. Oxidation and intramolecular ligand hydroxylation of $[Cu_2(mac)(CH_3CN)_2]^{2+}$.

No peroxido or bis-μ-oxido complex formation was detected during the oxidation reaction using low temperature stopped-flow techniques.[4c,4d] Kinetic studies revealed that

[a] Institut für Anorganische und Analytische Chemie, Justus-Liebig-Universität Gießen,
Heinrich-Buff-Ring 58, 35392 Gießen, Germany
Fax: +49-641-9934149
E-mail: siegfried.schindler@chemie.uni-giessen.de
[b] Department Chemie und Pharmazie, Anorganische Chemie, Universität Erlangen-Nürnberg,
Egerlandstraße 1, 91058 Nürnberg, Germany
[c] Department Chemie und Pharmazie, Organische Chemie, Universität Erlangen-Nürnberg,
Henkestraße 42, 91054 Nürnberg, Germany
Supporting information for this article is available on the WWW under http://dx.doi.org/10.1002/ejic.201000954.

the reaction most likely proceeds through a peroxido complex as an intermediate.[4c,4d] Furthermore, related complexes of $[Cu_2(mac)(CH_3CN)_2](ClO_4)_2$ were investigated. Here, no intramolecular ligand hydroxylation reactions were observed but bis-μ-oxido complexes were spectroscopically characterized.[5] Theoretical calculations confirmed the formation of different peroxido and oxido complexes as active species for these macrocyclic systems.[5–6] However, to date the mechanism of how a dicopper site binds and/or activates O_2, is far from being completely understood.[3o]

In order to investigate whether the dinuclearity of $[Cu_2(mac)(CH_3CN)_2](ClO_4)_2$ is crucial for the hydroxylation reaction, copper(I) complexes of the open-chain ligand (7*E*)-N^1-benzylidene-N^2-[(*E*)-2-(benzylideneamino)ethyl]ethane-1,2-diamine (**L¹**) (which resembles half of mac) were synthesized and characterized and their reactivity towards dioxygen was investigated. Additionally, the chemically reduced form of **L¹**, the amine N^1-benzyl-N^2-[2-(benzylamino)ethyl]ethane-1,2-diamine (**L²**) was synthesized and characterized (Scheme 1).

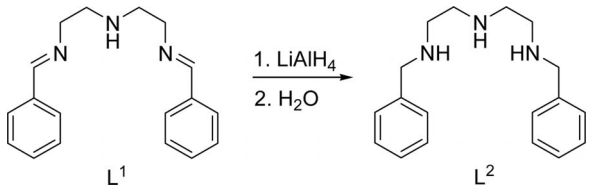

Scheme 1. Reduction of **L¹** to **L²**.

Results and Discussion

Syntheses and Characterization of L¹, 1 and 2

The reaction of benzaldehyde with diethylenetriamine in a 2:1 ratio yielded the Schiff Base ligand **L¹**, which shows an imine–aminal equilibrium in solution similar to its macrocyclic analogue.[4a–4c] Mac crystallizes in its monoaminal form.[4a,4b] An imine-aminal equilibrium in solution, and a preference for the aminal form in solid state are widely known for Schiff base ligands.[4b,5a,7] The ^1H NMR spectrum in $CDCl_3$ clearly demonstrates that the sample comprises 61% **L¹** in the aminal form and only 39% as the bisimine (Figure 2).

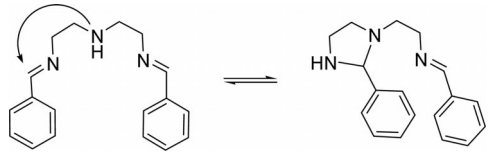

Figure 2. Imine-aminal equilibrium of **L¹**.

In solid state only the aminal form is found, as indicated by IR spectroscopy and X-ray analysis. The molecular structure of the animal form of **L¹** is shown in Figure 3. Within the crystal packing the molecules are stacked along the crystallographic *b* axis. Two stacks at a time are connected by intermolecular hydrogen bonds between the secondary amine groups N(1)–H(1)···N(1$^{\#1}$) [N(1)–H(1) 0.92(3) Å, H(1)···N(1$^{\#1}$) 2.55(3) Å, N(1)···N(1$^{\#1}$) 3.437(2) Å and N(1)–H(1)···N(1$^{\#1}$) 164(2)°; $-x + 1$, $y - 0.5$, $-z + 1$.]

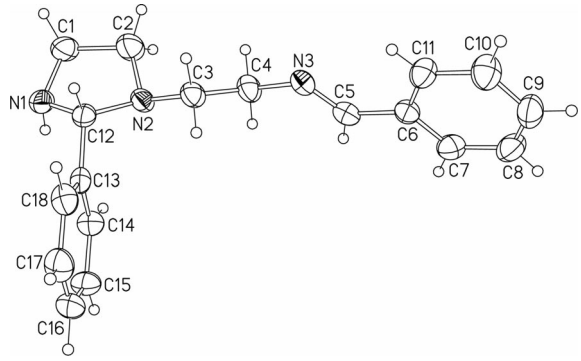

Figure 3. Thermal ellipsoid plot of the molecular structure of **L¹** (50% probability ellipsoids).

As expected, the reaction of **L¹** with $[Cu(CH_3CN)_4]PF_6$ yields the mononuclear complex $[Cu(\mathbf{L^1})(CH_3CN)]PF_6$ (**1**). The molecular structure of $[Cu(\mathbf{L^1})(CH_3CN)]^+$ with the atomic numbering scheme is shown in Figure 4. The copper(I) centre is coordinated in a distorted tetrahedral geometry by two imine donors, an amine donor and an acetonitrile molecule with a Cu–(N–) distance of 2.164(2) Å, Cu–(N=) distances of 2.044(2) and 2.086(2) Å and a Cu–(N≡) distance of 1.938(2) Å. The coordination sphere around the copper(I) centre is similar to that in $[Cu_2(mac)(CH_3CN)_2](ClO_4)_2$.[4c,4e] Complex **1** clearly resembles one half of $[Cu_2(mac)(CH_3CN)_2](ClO_4)_2$. However, the structure of **1** is less strained compared to its macrocyclic analogue. The N(2)–Cu(1)–N(3) angle is more than 15° and the N(1)–Cu(1)–N(100) angle more than 10° wider than those of $[Cu_2(mac)(CH_3CN)_2](ClO_4)_2$. Selected bond lengths [Å] and angles [°] for **1** are given in Table 1.

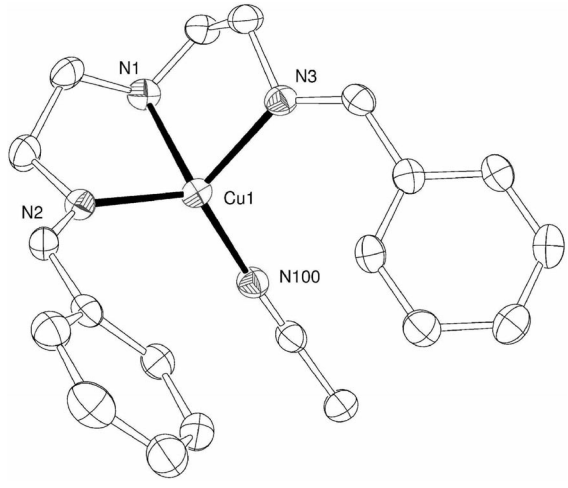

Figure 4. Molecular structure of the complex cation of **1**.

In contrast, and quite unexpectedly, we observed that when $[Cu(CH_3CN)_4]ClO_4$ was used instead of $[Cu(CH_3CN)_4]PF_6$ in the synthesis of the copper(I) complex, a helical dinuclear species, $[Cu_2(\mathbf{L^1})_2](ClO_4)_2$ (**2**), forms. The

Table 1. Selected bond lengths [Å] and angles [°] for **1**.

Bond lengths			
Cu(1)–N(100)	1.938(2)	Cu(1)–N(1)	2.164(2)
Cu(1)–N(2)	2.044(2)	Cu(1)–N(3)	2.086(2)
Bond angles			
N(100)–Cu(1)–N(2)	122.93(6)	N(2)–Cu(1)–N(1)	84.72(6)
N(100)–Cu(1)–N(3)	110.65(6)	N(3)–Cu(1)–N(1)	83.51(6)
N(2)–Cu(1)–N(3)	121.17(6)	C(100)–N(100)–Cu(1)	163.16(17)
N(100)–Cu(1)–N(1)	125.08(7)		

molecular structure of the cation of **2** with the atomic numbering scheme is presented in Figure 5 and selected bond lengths [Å] and angles [°] for **2** are given in Table 2.

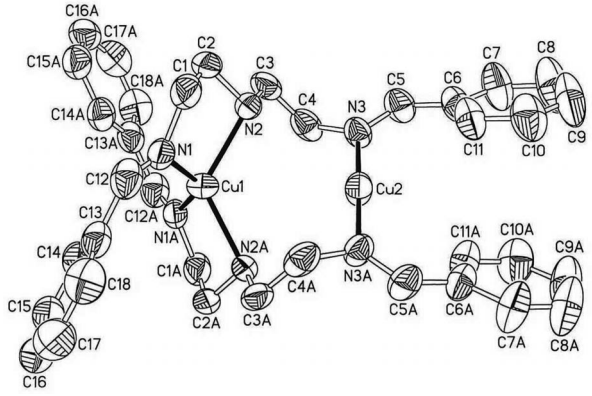

Figure 5. Thermal ellipsoid plot of the molecular structure of the complex cation of **2** (40% probability ellipsoids, C bound hydrogen atoms omitted for clarity).

Table 2. Selected bond lengths [Å] and angles [°] for **2**.

Bond lengths			
Cu(1)–N(1)	2.030(3)	Cu(1)–N(1A)[a]	2.030(3)
Cu(1)–N(2)	2.134(2)	Cu(1)–N(2A)[a]	2.134(2)
Cu(2)–N(3)	1.886(2)	Cu(2)–N(3A)[a]	1.886(2)
Bond angles			
N(1)–Cu(1)–N(1A)[a]	134.5(2)	N(1A)[a]–Cu(1)–N(2A)[a]	84.5(1)
N(1)–Cu(1)–N(2)	84.5(1)	N(2)–Cu(1)–N(2A)[a]	122.9(2)
N(1A)–Cu(1)–N(2)	117.8(1)	N(3A)[a]Cu(2)–N(3)	179.2(2)
N(1)–Cu(1)–N(2A)[a]	117.8(1)		

[a] Symmetry code: $-x + 2$, y, $-z + 1.5$.

The helical complex exhibits a crystallographic C_2 axis running through the two copper(I) centres. One copper(I) ion is coordinated in a distorted tetrahedral geometry by two imine donors with a Cu–N distance of 2.030(3) Å and two amine donors with a Cu–N distance of 2.134(2) Å. The second copper(I) centre shows linear coordination by two imine donors with a Cu–N distance of 1.886(2) Å, and weak interactions with two ClO_4^- counterions [Cu(2)···O(14) 2.927(3) Å]. The ClO_4^- counterions form hydrogen bonds to the N–H groups [N(2)–H(2)···O(14) with N(2)–H(2) 0.91 Å, H(2)···O(14) 2.26 Å, N(2)···O(14) 3.137(3) Å and N(2)–H(2)···O(14) 161°]. The separation of the two copper centres is 3.609(1) Å. Helical copper(I) complexes with Schiff base ligands are known[8] and a system with a macrocyclic ligand similar to mac has been described.[8a] However, most interesting is a comparison with a dicopper(I) helicate complex with a 2,6-bis(pyrazole-2-yl)pyridine derivative.[9] This ligand, which is totally different chemically to $\mathbf{L^1}$, shows some similarity if one overlaps their chemical formulae as shown in Scheme 2.

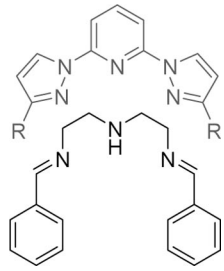

Scheme 2. Comparison of $\mathbf{L^1}$ with a 2,6-bis(pyrazole-2-yl)pyridine derivative (R = H, Me, *t*Bu).

That this comparison is not far fetched can be seen clearly in a comparison of **1** with the reported[9] complex $[\{Cu(\mu\text{-}L^{Mes})\}_2]^{2+}$. In both complexes there is a similar structural unit with one four- and one two-coordinate copper(I) ion.

Discussion of the Structure Dependence on the Counterion

The fact that the nature of the counterion has an important impact on the molecular structure is often observed in crystal-engineered coordination polymers, where the anion is part of the polymeric array.[10] Furthermore, counterions can have a strong influence on supramolecular structures. For example, Lehn showed that in some circular double helices where the counterion occupies the centre of the arrangement, the nature of the anion is responsible for the formation of either a cubic, a pentagonal or a hexagonal architecture.[11] Noncovalent interactions between a cation and a counterion might be crucial for the formation of various structure types. Silver terpyridyl and silver pyridyl thioether complexes form different aggregates, with the structure depending on the counterions and the solvents used.[12] It is suggested that weak interactions such as hydrogen bonding and X···H–C contacts play an important role in complex formation. Interestingly, and most recently, zwitterionic dicopper helicates with a salicylaldiminato unit as a ligand have been used for anion encapsulation studies.[8c]

The effect of counterions on the solid-state structure of metal compexes, e.g. on a thiourea-platinum(II) complex,[13] have been observed previously, however, to our knowledge, **1** and **2** are the first "simple" complexes where the nature of the non- or weakly coordinating counterions determines the complex structure in such a way. In general, noncovalent intramolecular and intermolecular interactions stabilize different species and are probably crucial for the formation of different complex structures. In **1**, one F···H–C interaction less than 2.55 Å and one weak intermolecular hydrogen bond with F(6)···H(1_2) 2.442 Å were observed per PF_6^- counterion. The helical complex **2** is stabilized by one

hydrogen bond per ClO_4^- counterion to the N–H group with a hydrogen acceptor distance of 2.26 Å. Furthermore, two O···H–C interactions less than 2.60 Å are apparent per ClO_4^- anion. The aromatic rings with C(6)–C(11) and C(6A)–C(11A) are not coplanar, and, with the closest distance of 3.774 Å between C(6) and C(11_2) of the neighbouring molecule, are not suitable for providing effective π-π interactions. Compounds **1** and **2** exhibit no striking differences concerning weak interactions with the exception of the stronger hydrogen bond in **2**. Therefore, crystallization and crystal packing effects might play a crucial role in structure formation. Crystal packing diagrams are presented in the supporting material.

Further Variation of the Counterions

To further investigate the influence of the counterion on the structure of the corresponding complexes, the copper(I) compounds with the counterions BF_4^- and SbF_6^- were synthesized in a similar way to **1**. Unfortunately, single crystals suitable for X-ray analyses were not obtained. However, mononuclear and dinuclear coordination types can be differentiated by spectroscopic methods. For example, the band arising from the N–H vibration of **1** appears at 3350 cm^{-1} in the IR (KBr) spectrum, whereas in **2** the wavenumber decreases to 3259 cm^{-1}, probably due to N–H···O hydrogen bonds between the N–H groups and ClO_4^-. Moreover, the presence or absence of MeCN signals in ^1H and ^{13}C NMR spectra establishes the formation of both the mononuclear and the dinuclear species.

For copper(I) complexes with a BF_4^- counterion, a band arising from the N–H vibration appears at 3268 cm^{-1} in the IR (KBr) spectrum similar to **2**, whereas in the ^1H and ^{13}C NMR spectra (measured in [D_6]DMSO) no signals for CH_3CN were found. These results indicate that $[Cu_2(\mathbf{L^1})_2](BF_4)_2$ was obtained during the reaction. For the copper(I) complex with a SbF_6^- counterion, however, the IR (KBr) spectrum exhibited two bands arising from N–H vibrations at 3286 and 3342 cm^{-1}, indicating the presence of both $[Cu_2(\mathbf{L^1})_2](SbF_6)_2$ and $[Cu(\mathbf{L^1})(CH_3CN)]SbF_6$ in the solid state. Integration of the MeCN signal in the ^1H NMR spectrum (measured in [D_6]DMSO) gives evidence that a mixture of $[Cu_2(\mathbf{L^1})_2](SbF_6)_2$ and $[Cu(\mathbf{L^1})(CH_3CN)]SbF_6$ was formed in a 4.6:1 ratio.

Thus, tetrahedral counterions such as ClO_4^- and BF_4^- prefer the formation of dinuclear species. Octahedral PF_6^- forms the mononuclear compound and SbF_6^- forms a mixture of mononuclear and dinuclear species. The dependence of the molecular structure on the counterion might be the result of packing effects in the solid state.

Investigation of the Behaviour of 1 and 2 in Solution

In order to investigate the behaviour of **1** and **2** in solution, various experiments were carried out. To study potential equilibria between **1** and **2**, low temperature NMR techniques were applied. Temperature-dependent ^1H NMR spectra of **1** and **2** in CD_3CN and [D_7]DMF were recorded down to –40 °C and –55 °C, respectively. The NMR spectra for both compounds were similar and differed only in the presence of the CH_3CN peak for **1**. Figure 6 shows the ^1H NMR spectra of **1** in CD_3CN at –40, –20, –10 and +25 °C. From the NMR patterns it is clear that for **1** and **2** only the mononuclear species is present in solution. Therefore, **2** decomposes into its mononuclear component in coordinating solvents.

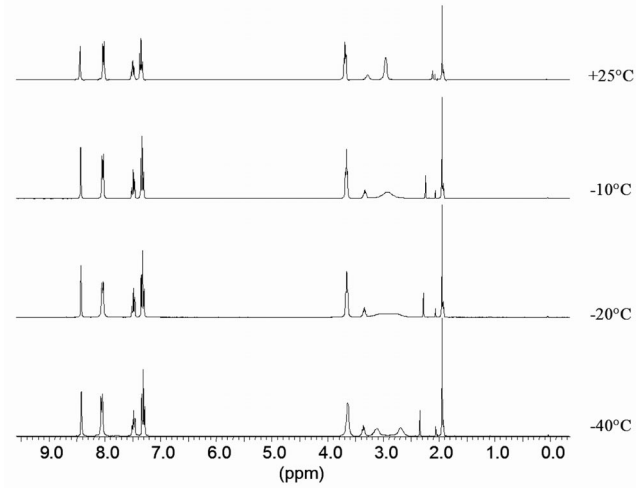

Figure 6. ^1H NMR spectra of $[Cu(\mathbf{L^1})(CH_3CN)]PF_6$ in CD_3CN at –40, –20, –10 and +25 °C.

^1H NMR spectra did not give any indication of equilibria between the dinuclear and mononuclear species as no significant line broadening was observed. Only the signal for the N–CH_2 protons split at about –20 °C into two broad signals at δ = 2.69 and 3.11 ppm, which show coalescence at about –10 °C. The signal splitting derives from the diastereotopy of the hydrogen atoms in the N–CH_2 groups, resulting in different chemical shifts. By raising the temperature, dissociation and subsequent association of the amine protons makes the diastereotopic hydrogen atoms chemically equivalent.

Low-temperature ^1H NMR spectroscopy of **1** and **2** in CD_3OD down to –80 °C gave different spectra for each complex. For **1**, NMR spectra were very similar to those obtained in coordinating solvents. For **2**, however, the ^1H NMR spectra showed line broadening from –20 °C onwards. Due to the limited solubility of **2** in weakly coordinating solvents, no deeper insight could be gained.

UV/Vis spectroscopy of **1** and **2** in CH_3CN also reveals that **2** forms a mononuclear species in coordinating solvents, as **2** yields an identical UV/Vis spectrum with ε values about twice as high as those of the mononuclear compound **1**. Further evidence for the decomposition of the dinuclear species by coordinating agents is given by the formation of $[Cu(\mathbf{L^1})(PPh_3)]ClO_4$ **(3)** from the reaction of **2** with PPh_3. The molecular structure of $[Cu(\mathbf{L^1})(PPh_3)]^+$ is shown in Figure 7. The copper(I) centre is coordinated in a distorted tetrahedral geometry by two imine donors, an amine donor and the phosphane ligand. The Cu–(N–)distance of

2.161(3) Å is practically identical to that in **1** [2.164(2) Å], whereas the Cu–(N=) distances of 2.092(3) and 2.112(3) Å are longer than those in **1** [2.044(2) and 2.086(2) Å], which is probably due to steric hindrance caused by the phosphane ligand. The Cu–P distance of 2.205(1) Å falls within the range usually observed. The steric demand of the phosphane ligand is also apparent in the shortened bond angles [N(1)–Cu(1)–N(2) 83.8(2)°, N(3)–Cu(1)–N(1) 109.6(2)° and N(3)–Cu(1)–N(2) 82.8(2)°]. Selected bond lengths [Å] and angles [°] for **3** are given in Table 3.

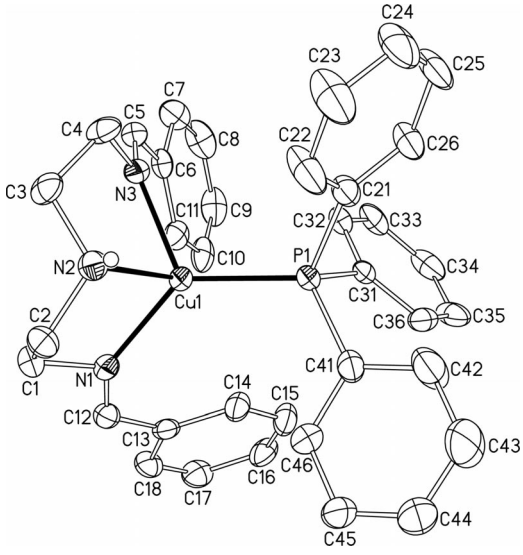

Figure 7. Thermal ellipsoid plot of the molecular structure of the complex cation of **3** (50% probability ellipsoids, C bound H atoms omitted for clarity).

Table 3. Selected bond lengths [Å] and angles [°] for **3**.

Bond lengths			
Cu(1)–N(1)	2.112(3)	Cu(1)–N(2)	2.161(3)
Cu(1)–N(3)	2.092(3)	Cu(1)–P(1)	2.205(1)
Bond angles			
N(3)–Cu(1)–N(1)	109.6(2)	N(3)–Cu(1)–P(1)	114.12(8)
N(3)–Cu(1)–N(2)	82.8(2)	N(1)–Cu(1)–P(1)	132.06(8)
N(1)–Cu(1)–N(2)	83.8(2)	N(2)–Cu(1)–P(1)	119.64(9)

From these results we can conclude that in coordinating solvents **1** and **2** form similar mononuclear copper(I) complexes. Potts et al. have previously reported related observations that a helical complex with a terpyridine derivative as a ligand shows different coordination behaviour in solution compared with the solid state.[14]

Electrochemistry

Cyclic voltammetry of **1** and **2** was performed with a scan rate of 100 mV s^{-1} in CH_3CN. Both compounds exhibited the same electrochemical behaviour with an irreversible Cu^{I}/Cu^{II} redox couple with $E_{1/2}$ = +0.12 V (E_{pa} = +0.19 V, E_{pc} = +0.04 V, $j_{pa/pc}$ = 0.46). An additional irreversible reduction peak with E_{pc} = –0.16 V was observed. This peak could be assigned to the reduction of a decomposition product of the copper(II) species. In contrast, $[Cu_2(mac)(CH_3CN)_2](ClO_4)_2$ exhibits one irreversible oxidation peak with E_{pa} = 0.12 V. E_{pa} in $[Cu_2(mac)(CH_3CN)_2](ClO_4)_2$, which is shifted by 70 mV to more negative potentials compared to **1**, although both complexes exhibit a similar coordination sphere. The E_{pa} shift could be explained by differences in the wider chemical environment of the copper(I) centres in both complexes.

Copper(II) Complexes

In order to compare the oxidation behaviour of **1** with $[Cu_2(mac)(CH_3CN)_2](ClO_4)_2$, **1** was treated with dioxygen in different solvents. Oxidation of **1** in CH_3OH yielded the bismethoxido bridged species $[Cu_2(\mathbf{L^1})_2(OCH_3)_2](PF_6)_2$ (**4**), whereas in CH_2Cl_2 $[Cu_2(\mathbf{L^1})_2(OH)_2](PF_6)_2$ (**5**) was formed. The molecular structure of $[Cu_2(\mathbf{L^1})_2(OCH_3)_2]^{2+}$ with the atomic numbering scheme is shown in Figure 8, and selected bond lengths [Å] and angles [°] for **4** are given in Table 4.

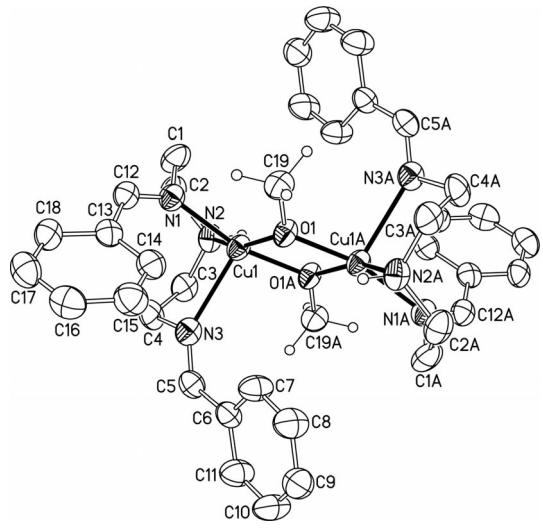

Figure 8. Thermal ellipsoid plot of the molecular structure of the complex cation of **4** (50% probability ellipsoids, C bound H atoms of the ligand omitted for clarity).

Table 4. Selected bond lengths [Å] and angles [°] for **4**.

Bond lengths			
Cu(1)–N(1)	2.019(5)	Cu(1)–O(1)	1.936(4)
Cu(1)–N(2)	2.073(4)	Cu(1)–O(1A)[a]	1.940(4)
Cu(1)–N(3)	2.365(5)	Cu(1)–Cu(1A)[a]	3.013(2)
Bond angles			
O(1)–Cu(1)–O(1A)[a]	78.0(2)	O(1A)[a]–Cu(1)–N(2)	95.1(2)
O(1)–Cu(1)–N(1)	99.3(2)	N(1)–Cu(1)–N(2)	82.0(2)
O(1A)[a]–Cu(1)–N(1)	164.8(2)	O(1)–Cu(1)–N(3)	120.0(2)
O(1)–Cu(1)–N(2)	158.7(2)		

[a] Symmetry code: $-x + 1, -y, -z + 1$.

In dinuclear **4** each copper(II) ion is coordinated in a distorted square pyramidal geometry with τ = 0.108 (τ = 0 for a square pyramidal, τ = 1 for a trigonal bipyramidal

complex).[15] The copper centres are related to one another by a centre of inversion. The base of the pyramid is formed by N(1), N(2), O(1) and O(1A), and N(3) forms the top of the pyramid. Compared to **1**, the Cu(1)–N(1) and Cu(1)–N(2) distances are shorter at 2.019(5) and 2.073(4) Å [2.044(2) and 2.164(2) Å in **1**], respectively, whereas the Cu(1)–N(3) distance is significantly increased at 2.365(5) Å compared to 2.086(2) Å in **1**. The Cu(1)–O(1) and Cu(1)–O(1A) distances are relatively short at 1.936(4) and 1.940(4) Å, respectively. The Cu(1)–Cu(1A) distance of 3.013(2) Å is normal compared to related complexes. The PF_6^- counterions are involved in hydrogen bonding with the N–H groups [N(2)–H(2)···F($14^{\#1}$) with N(2)–H(2) 0.92, H(2)···F$14^{\#1}$ 2.28 and N(2)···F($14^{\#1}$) 3.199(7) Å, and N(2)–H(2)···F($14^{\#1}$) 176°, $-x + 1, -y, -z + 1$]. The molecular structure is related to the analogous bismethoxido bridged species obtained during the oxidation of $[Cu_2(mac)(CH_3CN)_2](ClO_4)_2$ in a mixture of solvents containing acetonitrile.[16] Here Rieger and coworkers demonstrated that $[Cu_2(mac)(CH_3CN)_2](ClO_4)_2$ does not always undergo intramolecular ligand hydroxylation and thus obtained the first bismethoxido bridged copper(II) complex as an oxidation product.

The molecular structure of $[Cu_2(\mathbf{L^1})_2(OH)_2]^{2+}$ (**5**) with the atomic numbering scheme can be seen in Figure 9, and selected bond lengths [Å] and angles [°] **5** are given in Table 5. In the dinuclear complex each copper(II) ion is coordinated in a square pyramidal geometry with $\tau = 0.046$.

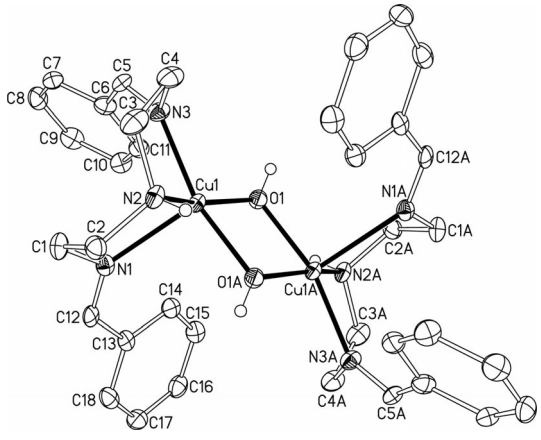

Figure 9. Thermal ellipsoid plot of the molecular structure of the complex cation of **5** (50% probability ellipsoids, C bound H atoms omitted for clarity).

The copper(II) centres are related to each other by a centre of inversion on the Cu(1)–Cu(1A) axis. Both pyramids share the O(1)–O(1A) edge analogous to **4**. The base of the pyramid is formed by N(2), N(3), O(1) and O(1A), and N(1) forms the top of the pyramid. Compared to **4**, Cu(1)–N(1), Cu(1)–O(1) and Cu(1)–N(2) distances are slightly shorter at 2.320(3), 1.928(3) and 2.038(3) Å. The Cu(1)–N(3) distance is similar to that of **4** at 2.020(3) Å, and the Cu(1)–O(1A) distance is slightly longer at 1.957(2) Å. Similar to **4**, the formation of hydrogen bonds between the N–H group of the ligand and the PF_6^- anion is observed:

Table 5. Selected bond lengths [Å] and angles [°] for **5**.

Bond lengths			
Cu(1)–N(1)	2.320(3)	Cu(1)–O(1)	1.928(3)
Cu(1)–N(2)	2.038(3)	Cu(1)–O(1A)[a]	1.957(3)
Cu(1)–N(3)	2.020(3)	Cu(1)–Cu(1A)[a]	2.9846(9)
Bond angles			
O(1)–Cu(1)–O(1A)[a]	79.6(2)	O(1A)[a]–Cu(1)–N(2)	92.3(2)
O(1)–Cu(1)–N(3)	99.2(2)	N(3)–Cu(1)–N(2)	82.9(2)
O(1A)[a]–Cu(1)–N(3)	162.5(2)	O(1)–Cu(1)–N(1)	116.7(2)
O(1)–Cu(1)–N(2)	159.7(2)		

[a] Symmetry code: $-x + 1, -y + 1, -z + 1$.

N(2)–H(2)···F(12) with N(2)–H(2) 0.93, H(2)···F(12) 2.18 and N(2)···F(12) 3.058(4) Å, and N(2)–H(2)···F(12) 158°, and with the alternative position of the distorted PF_6^- anion: N(2)–H(2)···F(15A) with N(2)–H(2) 0.93, H(2)···F(15A) 2.60, N(2)···F(15) 3.23(2) Å and N(2)–H(2)···F(15A) 126°.

Investigation of the Oxidation Reaction

Due to the molecular structures of the copper(II) compounds, no hydroxylation of the ligand was observed during the oxidation of **1** in MeOH or CH_2Cl_2. However, as yields for **4** and **5** were quite low at 73% and 58%, a further experiment was performed to investigate potential ligand hydroxylation. Complex **1** was treated with dioxygen in CH_2Cl_2, and the copper(II) ions were removed with NH_3. The remaining organic residue consisted of $\mathbf{L^1}$ and its decomposition product benzaldehyde. No hydroxylation of $\mathbf{L^1}$ was observed in any reaction.

In order to detect a dioxygen adduct of these complexes, such as a peroxido or superoxido species, during the oxidation of **1** in CH_2Cl_2, the reaction was probed with low temperature stopped-flow investigations. This technique has been quite useful in the past to observe such reactive intermediates.[3l,3m,17] In up to 41 s total time, time resolved spectra did not show any changes in absorption at temperatures between –88 °C and –3 °C. The oxidation reaction proceeded very slowly, and no spectroscopic detection of any reactive dioxygen adduct was possible.

In order to draw conclusions about the intermediates formed during the oxidation reaction, a chemical approach was chosen. Nucleophilic peroxido compounds can be protonated by acids at the peroxido moiety to give H_2O_2. In reverse, the detection of H_2O_2 should indicate previous formation of a peroxido species. When **1** was oxidized in CH_2Cl_2 at –40 °C and the reaction quenched with HPF_6, an average amount of 7.8% H_2O_2 was found by iodometric titration. Formation of H_2O_2 could also be verified by using H_2O_2 test strips.

During investigations of the oxidation reaction we found that the absorption spectrum of a freshly oxidized solution of **1** in CH_2Cl_2 differs from the spectrum of **5**. Therefore, a compound other than **5** was the first "stable" product formed in the oxidation reaction. IR spectra of the oxidized solution did not show any bands belonging to an OH vi-

bration, and in the field desorption mass spectrum (FD-MS) a peak at *m/z* = 357 corresponding to the $[Cu(\mathbf{L^1})O]^+$ fragment was observed. Thus, we assume that the oxido compound $[Cu_2(\mathbf{L^1})_2O]^{2+}$ was formed. Further evidence was given by monitoring the reaction of a freshly oxidized solution of **1** in CH_2Cl_2 with one equivalent of H_2O by UV/Vis spectroscopy. Absorption spectra clearly indicated the formation of **5** [shoulder, λ_{max} = 582 nm (473)] from $[Cu_2(\mathbf{L^1})_2O]^{2+}$ [λ_{max} = 594 nm (185)] as shown in Figure 10. Copper oxido complexes have been recently described to most likely be an active species in the selective oxidation of methane to methanol catalyzed by methane monooxygenase.[18]

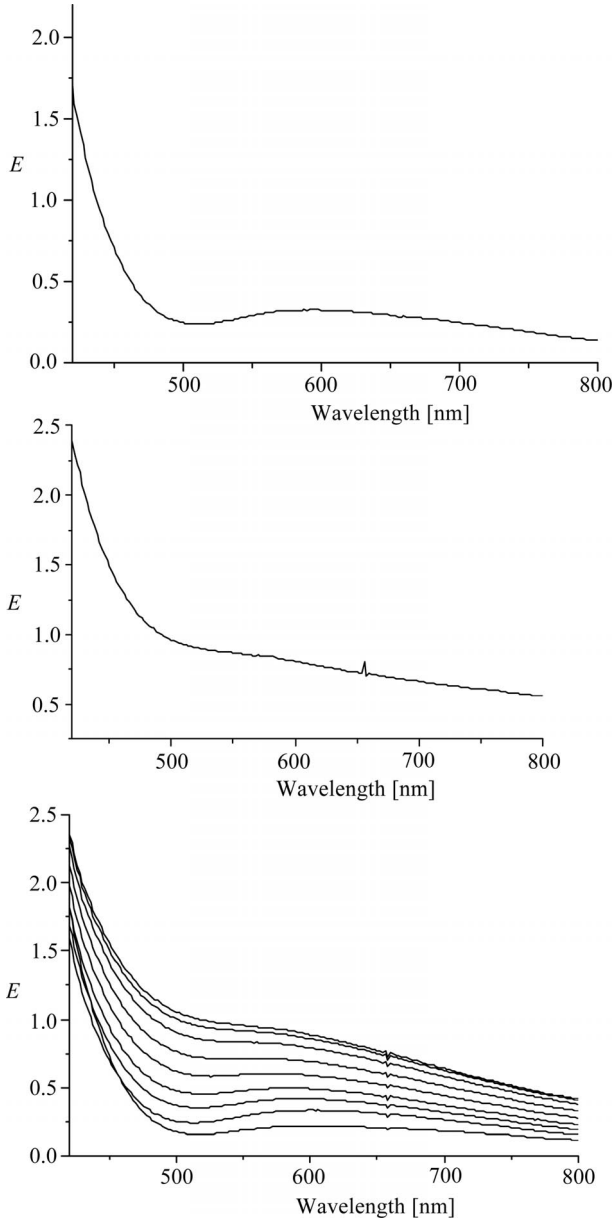

Figure 10. Top: UV/Vis spectrum of an oxidized solution of **1** in CH_2Cl_2; middle: UV/Vis spectrum of **5** in CH_2Cl_2; bottom: time-resolved UV/Vis spectra of an oxidized solution of **1** in CH_2Cl_2, quenched with one equivalent of water.

Complex **1** reacts slowly with dioxgen, probably forming a peroxido species and the oxido compound $[Cu_2(\mathbf{L^1})_2O]^{2+}$ prior to the bishydroxido-bridged complex **5**. In contrast, macrocyclic $[Cu_2(mac)(CH_3CN)_2](ClO_4)_2$ reacts much faster with dioxygen to give a peroxido intermediate. The peroxido intermediate decays by hydroxylation of the ligand.[4c,4d] The higher reactivity of $[Cu_2(mac)(CH_3CN)_2](ClO_4)_2$ towards dioxygen might be attributed to its more negative redox potential and its highly preorganized structure. Dioxygen might fit very well between the two copper(I) centres, and because of the proximity to the aromatic spacer, hydroxylation of the ligand is possible. In **1** there is no preorganization present, and the aromatic moieties of the ligand are much more flexible. These differences might be responsible for the very different oxidation behaviour. These findings are not completely unexpected because similar observations were made previously for an important model compound, $[Cu_2(XYL\text{-}H)]^{2+}$. This dinuclear copper(I) complex shows hydroxylation of the aromatic spacer group upon reaction with dioxygen.[3e,3j–3m] Kinetic studies of the oxidation process reveal that the reaction probably proceeds through a peroxido intermediate.[3l,3m] In contrast, here the mononuclear copper(I) compound containing "half" of the XYL-H ligand did not show any hydroxylation of the ligand upon oxidation.[3e,19] However, other mononuclear copper(I) complexes exhibit aromatic as well as aliphatic ligand hydroxylation when reacted with dioxygen.[20]

Copper Complexes with $\mathbf{L^2}$

From our previous work we know that it can be difficult to observe copper dioxygen adducts as reactive intermediates when Schiff bases are used as ligands.[4c,4e,17b,21] Therefore we have also synthesized $\mathbf{L^2}$, the amine derivative of the imine $\mathbf{L^1}$. $\mathbf{L^2}$ has been described previously as a hydrochloride salt.[22] We used $LiAlH_4$ instead of $NaBH_4$ for the reduction of $\mathbf{L^1}$ to $\mathbf{L^2}$ to avoid an acid workup.

It is quite difficult − mainly due to disproportionation reactions − to isolate copper(I) amine complexes as solids and/or to structurally characterize them. Therefore, we were not surprised that, similar to our recent work on ligands related to $\mathbf{L^2}$,[23] only dilute solutions of copper(I) $\mathbf{L^2}$ complexes could be prepared in situ by mixing the amine with $[Cu(CH_3CN)_4]PF_6$ in different solvents.

^1H NMR spectroscopy in $[D_6]$DMSO supports the presence of a highly symmetrical copper(I) complex in solution. A singlet at δ = 2.07 ppm is observed from the methyl protons of CH_3CN. This could be either caused by a fast exchange between coordinated and free acetonitrile or it could mean that CH_3CN is not coordinated at all. Unfortunately, it is not possible to distinguish between these two possibilities from these measurments, because the downfield shift of the signal for the methyl protons compared to that of the free CH_3CN is too small to be significant. However, we assume from previous studies that acetonitrile is coordinated in solution and the complex should be formulated as

$[Cu(\mathbf{L^2})(CH_3CN)]PF_6$. The coordination of $\mathbf{L^2}$ to the copper ion mainly affects the chemical shift of the NH protons. These appear with a downfield shift of about 1.5 ppm at δ = 3.49 ppm compared to free $\mathbf{L^2}$. The CH_2 groups of the ethyl bridges and the benzyl groups show singlets at δ = 2.64 and 3.73 ppm, respectively. The aromatic protons show a multiplet at 7.27–7.37 ppm. ^{13}C NMR spectroscopy exhibits only one set of signals for CH_3CN, at 0.00 and 116.92 ppm, which is shifted only about 0.5 ppm upfield compared with that of free CH_3CN. Again, this shift is not significant enough to prove or exclude coordination of CH_3CN. Additional signals at δ = 45.88 and 47.70 ppm for the CH_2 groups of the ethyl bridges, δ = 53.20 ppm for the benzylic CH_2 groups and δ = 126.09, 127.20, 127.51 and 138.06 ppm for the aromatic C atoms support the C_S symmetry of the complex. Furthermore, coordination of $\mathbf{L^2}$ to the copper(I) ion is characterized with the observation of a peak at m/z = 346 (100%) for the fragment $[Cu(\mathbf{L^2})]^+$ in FD-MS measurements in CH_3CN. An additional peak at m/z = 284 (20%) corresponding to $\mathbf{L^2}$ is also seen. UV/Vis spectroscopy of a complex synthesized in situ measured in CH_3CN solution revealed two bands at 214 (ε = 17.301 $M^{-1}cm^{-1}$) and 242 nm (shoulder, ε = 6.863 $M^{-1}cm^{-1}$). These bands can be assigned to intraligand transitions.

Electrochemistry of $[Cu(\mathbf{L^2})(CH_3CN)]PF_6$

Electrochemical measurements were performed with equimolar solutions of $[Cu(CH_3CN)_4]PF_6$ and $\mathbf{L^2}$ (1:1) in CH_3CN. Figure 11 shows the cyclic voltammogram of this solution with v = 50, 100 and 200 mV s^{-1}. The Cu^I/Cu^{II} redox behaviour of this complex is quasireversible with $E_{1/2}$ = +0.02 V for v = 100 mV s^{-1} (E_{pa} = +0.10 V, E_{pc} = –0.07 V) and $j_{pa/pc}$ = 1.04. Compared with **1** described above, the redox potential has shifted to a value about 0.5 V more negative. Thus, $[Cu(\mathbf{L^2})(CH_3CN)]PF_6$ is thermodynamically less stable and can be oxidized more easily than **1**.

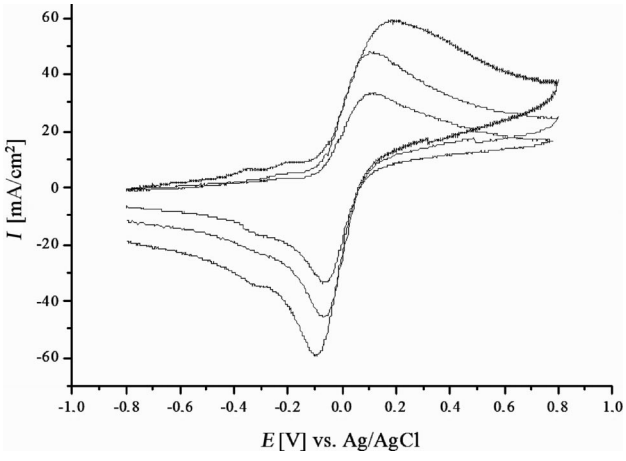

Figure 11. Cyclic voltammetry of a 1:1 mixture of $[Cu(CH_3CN)_4]PF_6$ and $\mathbf{L^2}$ in CH_3CN (v = 50, 100, 200 mV s^{-1}).

Previously, correlations have been made for some copper(I) compounds with regard to the basicity of the ligands and the resulting redox potentials of the complexes.[17c] An increase in ligand basicity caused by a shift of the redox potentials towards more negative values. Assuming that $[Cu(\mathbf{L^2})(CH_3CN)]PF_6$ has the same coordination geometry as **1**, we can explain the shift of the redox potential towards more negative values with the increased basicity of $\mathbf{L^2}$.

Investigation of the Oxidation Reaction of $[Cu(\mathbf{L^2})(CH_3CN)]PF_6$

The reaction of the $[Cu(\mathbf{L^2})(CH_3CN)]PF_6$ with dioxygen was investigated in CH_2Cl_2 at –88 °C, –41 °C and –3 °C, using stopped-flow techniques as described above. Dioxygen adduct complexes were not detected spectroscopically under these conditions. Again this was unsurprising because we have previously observed copper(I) complexes with related tridentate ligands, and these reactive intermediates can be detected only in a few cases.[23b] Therefore, no further detailed kinetic measurements were performed on this system.

$[Cu_2(\mathbf{L^2})_2Cl_3]PF_6 \cdot 2$ MeOH (6)

It has been shown previously that a copper(II) chlorido complex is an acceptable structural analogue of a copper dioxygen adduct complex.[17b] Therefore, a chloridocopper(II) complex with $\mathbf{L^2}$ as ligand was prepared and structurally characterized. The crystal structure of the cation of $[Cu_2(\mathbf{L^2})_2Cl_3]PF_6 \cdot 2MeOH$ (**6**) is presented in Figure 12. Both copper(II) ions in the dinuclear complex show distorted square pyramidal geometry (with a τ-value of 0.09) and are coordinated by three amine and two chloride donors. Both pyramids are linked by the axial chloride anion Cl(1) with Cu(1)–Cl(1) 2.5874(8) Å, Cl(1)–Cu(1)–Cl(2) 104.49(3)° and Cu(1)–Cl(1)–Cu(1A) 110.62(5)°. The base of

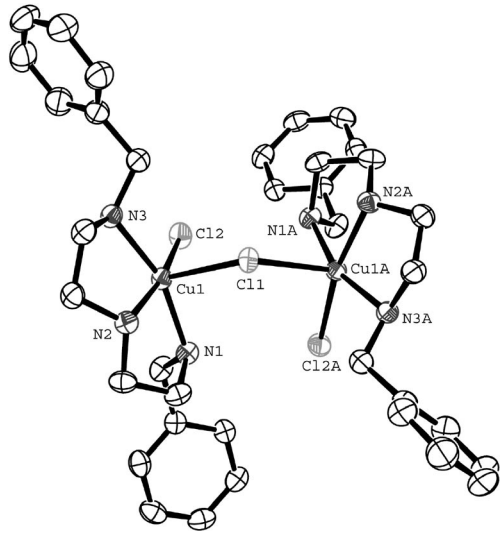

Figure 12. Molecular structure of the complex cation of **6**.

both pyramids is formed by N(1), N(2), N(3) and Cl(2) with N(1)–Cu(1)–N(2) 84.57(11)°, N(2)–Cu(1)–N(3) 83.20(11)°, N(3)–Cu(1)–Cl(2) 93.47(8)° and N(1)–Cu(1)–Cl(2) 95.26(8)°. The separation of the two copper centres is relatively short at 4.255 Å, whereas the copper amine donor distances between 2.021(3) and 2.060(3) Å compare well with similar copper complexes.[24] From the molecular structure it is obvious that a dinuclear peroxido or oxido complex can (and most likely will) form during the reaction of $[Cu(\mathbf{L^2})(CH_3CN)]PF_6$ with dioxygen. However, due to kinetic reasons we were unable to detect such an intermediate spectroscopically.[4c,4d,21,23b]

Conclusions

The new tridentate ligand $\mathbf{L^1}$ provides a wide range of copper(I) and -(II) complexes. Cu(I) complexes of $\mathbf{L^1}$ display an unusual anion effect. With a PF_6^- counterion, the mononuclear copper(I) complex $[Cu(\mathbf{L^1})(CH_3CN)]PF_6$ (**1**) was formed, whereas the reaction of $\mathbf{L^1}$ with $[Cu(CH_3CN)_4]ClO_4$ produced the dinuclear helical compound $[Cu_2(L^1)_2](ClO_4)_2$ (**2**). The formation of different molecular structures is probably caused by crystallization effects as well as the stronger hydrogen bond in **2**. No other striking differences concerning weak interactions were found for either of the complexes.

In coordinating solvents, the dinuclear compound changed into the mononuclear species. This finding was supported by the formation of $[Cu(\mathbf{L^1})(PPh_3)]ClO_4$ (**3**) in the reaction of **2** with PPh_3.

Oxidation of **1** with dioxygen in CH_3OH and CH_2Cl_2 yielded the dinuclear complexes $[Cu_2(\mathbf{L^1})_2(OCH_3)_2](PF_6)_2$ (**4**) and $[Cu_2(\mathbf{L^1})_2(OH)_2](PF_6)_2$ (**5**). No hydroxylation of the ligand was observed upon oxidation. The oxidation behaviour differs from that of the dinuclear compound $[Cu_2(mac)(CH_3CN)_2](ClO_4)_2$. Reasons behind the different reactivity could be seen in the higher redox potential of **1** and the absence of a dinuclear copper core providing a highly preorganized system. Investigation of reaction intermediates during oxidation showed that a peroxido species as well as the oxido compound $[Cu_2(\mathbf{L^1})_2O](PF_6)_2$ most likely were formed during the reaction. However, detection of the peroxido species by UV/Vis spectroscopy was not possible. Furthermore, the reaction of $[Cu(\mathbf{L^2})(CH_3CN)]PF_6$ with dioxygen was investigated. Again, we could not detect the presence of a dioxygen adduct spectroscopically. A dinuclear copper(II) complex, $[Cu_2(\mathbf{L^2})_2Cl_3]PF_6$, was prepared and structurally characterized.

Experimental Section

Materials and Methods: Commercially available reagents and solvents used were of reagent quality. Organic solvents used in the syntheses of the copper(I) complexes were dried according to standard procedures. Diethylenetriamine and benzaldehyde were distilled prior to use. $[Cu(CH_3CN)_4]X$ (X = ClO_4, PF_6, BF_4, SbF_6) salts were synthesized according to literature procedures.[25] Preparation and handling of air-sensitive compounds were carried out in a glove box filled with argon (MBraun, Germany; water and dioxygen less than 1 ppm).

^1H and ^{13}C NMR spectra were recorded with a DXP 300 AVANCE spectrometer. For low-temperature measurements of **1** and **2** in $[D_7]DMF$, a Bruker DRX 400 AVANCE spectrometer was used. IR spectra were recorded in solution or as KBr pellets with a ATJ Mattson Infinity 60 AR-FT-IR instrument. Elemental analyses were carried out with a Carlo–Erba Element Analyser Model 1106 and FD mass spectra were measured with a JEOL JMS 700 instrument at 70 eV and a source temperature of 200 °C. For standard UV/Vis spectroscopic investigations and for the investigation of the reaction of an oxidized solution of **1** with H_2O, a Hewlett–Packard 8452A diode array spectrophotometer was used. Time-resolved UV/Vis spectra of the reaction of **1** with dioxygen were recorded with a modified Hi-Tech SF-3L low-temperature stopped-flow unit (Salisbury, U.K.) equipped with a J&M TIDAS 16–500 photodiode array spectrophotometer (J&M, Aalen, Germany).[26] Using syringes, an in situ prepared 4×10^{-4} M solution of **1** was transferred to the low-temperature stopped-flow instrument. A dioxygen saturated solution was prepared by bubbling O_2 through CH_2Cl_2 in a syringe (solubility of O_2 at 25 °C in CH_2Cl_2: 3.8×10^{-3} M).[27] Cyclic voltammetry was carried out using an EG&G Model 263 potentiostat. The measurements were performed at 25 °C under nitrogen in CH_3CN or DMSO solutions containing 0.1 M nBu$_4$NPF$_6$ and 1×10^{-3} to 10^{-4} M copper(I) complex. The experiments utilized a two-chambered electrochemical H-cell in which the working solution compartment was separated from the other by a fine glass frit. The reference electrode for the electrochemical measurements was an Ag/AgCl electrode (BAS MF-1052). A glassy carbon disk was used as the working electrode and a coiled platinum wire was used as the reference electrode. Potentials are reported relative to the ferrocene/ferrocenium couple (+0.42 V vs. Ag/AgCl).

X-ray Structure Determination of $\mathbf{L^1}$ and 1–6: Single crystals were coated with protective perfluoropolyether oil and mounted on a glass fibre. Data for $\mathbf{L^1}$, **2** and **4** were collected with a Siemens P4 diffractometer at 210(2), 295(2) and 210(2) K and for **1**, **3**, **5** and **6** with a Nonius Kappa CCD diffractometer at 173(2), 100(2) and 100(2) K, respectively (Mo-K_α, λ = 0.71073 Å, each graphite-monochromated). Space groups were determined from systematic absences. All structures were solved by direct methods and refined on F^2 using full-matrix least-squares techniques.[28] All non-hydrogen atoms were refined with anisotropic thermal parameters (see Tables 6 and 7).

For all compounds, data were corrected for Lorentz and polarization effects. An empirical absorption correction using SCALEPACK was carried out for **1**. Pure organic $\mathbf{L^1}$ absorption effects were neglected. Semiempirical absorption corrections on the basis of Psi-scans were performed for **2** and **4**, and a semiempirical absorption correction on the basis of multiple scans using SORTAV[29] was carried out for **3**. A numerical absorption correction based on the indexing of crystal faces was performed for **5**. Hydrogen atoms of **6** where treated using a riding model. Hydrogen atoms of $\mathbf{L^1}$ were located from a difference Fourier map and refined with individual isotropic displacement parameters. With the exception of the O1 bound hydrogen atom H1 of **5**, whose position was derived from a difference fourier map, all hydrogen atoms of compounds **2**, **3**, **4** and **5** were placed in positions of optimized geometry and their displacement parameters were tied to the equivalent isotropic displacement parameters of the corresponding carrier atoms by a factor of 1.2 or 1.5.

Due to of the absence of heavy atoms, the absolute structure of $\mathbf{L^1}$ was not determined. Hydrogen atoms of **1** were located from a

Table 6. Crystal data and structure refinement for **L[1]**, **1** and **2**.

Compound	**L[1]**	**1**	**2**
Empirical formula	$C_{18}H_{21}N_3$	$C_{20}H_{24}N_4CuPF_6$	$C_{36}H_{42}N_6Cu_2Cl_2O_8$
Formula weight	279.38	528.94	884.74
Temperature [K]	210(2)	173(2)	295(2)
Wavelength [Å]	0.71073	0.71073	0.71073
Space group	$P2_1$	$P\bar{1}$	$C2/c$
a [Å]	8.947(1)	8.8145(2)	16.763(1)
b [Å]	5.515(1)	11.2443(2)	15.213(1)
c [Å]	16.088(2)	12.2806(2)	17.344(1)
α [°]	90	110.282(1)	90
β [°]	98.93(1)	91.682(1)	116.44(1)
γ [°]	90	95.242(1)	90
Volume [Å^3]	784.2(2)	1134.49(4)	3960.3(5)
Z	2	2	4
Density, calcd. [Mg m^{-3}]	1.183	1.534	1.484
Absorption coeff. [mm^{-1}]	0.071	1.548	1.266
R indices [$I > 2\sigma(I)$]	$R_1 = 0.0405$	$R_1 = 0.0337$	$R_1 = 0.0462$
	$wR_2 = 0.0805$	$wR_2 = 0.0873$	$wR_2 = 0.0796$
R indices (all data)	$R_1 = 0.0629$	$R_1 = 0.00468$	$R_1 = 0.1047$
	$wR_2 = 0.0892$	$wR_2 = 0.0934$	$wR_2 = 0.0956$

Table 7. Crystal data and structure refinement for **3**, **4** **5**.

	3	**4**	**5**
Empirical formula	$C_{37.5}H_{39}N_3CuCl_{1.33}PO_{4.33}$	$C_{38}H_{48}N_6O_2Cu_2P_2F_{12}$	$C_{42}H_{56}N_6O_4Cu_2P_2F_{12}$
Formula weight	742.83	1037.84	1125.95
Temperature [K]	100(2)	210(2)	100(2)
Wavelength [Å]	0.71073	0.71073	0.71073
Space group	$R\bar{3}$	$P2_1/n$	$P\bar{1}$
a [Å]	35.126(1)	9.074(1)	9.4575(4)
b [Å]	35.126(1)	11.193(1)	10.6958(5)
c [Å]	15.4896(5)	21.017(3)	12.4593(7)
α [°]	90	90	101.657(4)
β [°]	90	92.75(1)	92.168(4)
γ [°]	120	90	104.018(3)
Volume [Å^3]	16550.7(9)	2132.1(4)	1192.6(1)
Z	18	2	1
Density, calcd. [Mg m^{-3}]	1.342	1.617	1.568
Absorption coeff. [mm^{-1}]	0.778	1.168	1.053
R indices [$I > 2\sigma(I)$]	R_1[a] = 0.0553	R_1[a] = 0.0615	R_1[a] = 0.0501
	$wR_2 = 0.1270$	$wR_2 = 0.1201$	$wR_2 = 0.0834$
R indices (all data)	$R_1 = 0.1070$	$R_1 = 0.1309$	$R_1 = 0.0933$
	$wR_2 = 0.1577$	$wR_2 = 0.1478$	$wR_2 = 0.0954$

[a] $R_1(F_o) = \Sigma||F_o| - |F_c||/\Sigma|F_o|$; $wR_2(F_o^2) = (\Sigma[w(F_o^2 - F_c^2)^2]/\Sigma[w(F_o^2)^2])^{1/2}$.

difference Fourier map and refined with isotropic displacement parameters. Positional parameters were refined while one mutual isotropic displacement parameter was kept fixed during refinement. In the crystal structure of **3**, solvent molecules (best described as CH_2Cl_2 and THF) were distorted around the crystallographic C_3 axis. For these molecules, no hydrogen atoms were taken into account during refinement. The PF_6^- counterion of **4** in the equatorial plane and the PF_6^- counterions of **5** were distorted. Two alternative positions were refined with occupancies of 87.1(6)% for F(11)–F(14) and 12.9(6)% for F(11A)–F(14A) in the case of **4** and of 75.9(4)% for F(13)–(16) and 24.1(4)% for F(13A)–F(16A) in the case of **5**. The structure **5** included two acetone molecules per copper(II) complex unit. Complex **6** included two MeOH molecules per copper(II) complex unit.

Syntheses of Ligands and Complexes

Caution! Perchlorate salts are potentially explosive and should be handled with great care!

(7*E*)-*N*[1]-Benzylidene-*N*[2]-[(*E*)-2-(benzylideneamino)ethyl]ethane-1,2-diamine (L[1]): L[1] was synthesized by a modified literature procedure.[22] A solution of benzaldehyde (4.25 g, 40.0 mmol) and diethylenetriamine (2.06 g, 20.0 mmol) in $CHCl_3$ (300 mL) was heated to reflux for 3 h. The resulting yellow solution was washed with H_2O (50 mL), and the organic layer was dried with Na_2SO_4. Evaporation of the solvent yielded a yellow oil that was crystallized from hot CH_3CN containing charcoal. The product was obtained as a white solid in 63% yield (3.50 g). Colorless single crystals suitable for X-ray diffraction studies were obtained from recrystallisation of the crude product from CH_3CN at –20 °C. $C_{18}H_{21}N_3$ (279.38): calcd. C 77.38, H 7.57, N 15.04; found C 77.48, H 8.22, N 15.07. ^{1}H NMR (300 MHz, $CDCl_3$): δ = 1.91 (s, 1 H, N–H), 2.52–2.59 (m, 2 H, CH_2–N_{tert} in the aminal), 2.91–3.01 (m, 2 and 4 H, CH_2–N– in the aminal and the bisimine), 3.23–3.46 (m, 2 H, CH_2–N_{sec} in the aminal), 3.76 (m, 2 and 4 H, CH_2–N= in the aminal and the bisimine), 4.16 (s, 1 H, C–H in the aminal), 7.26–7.67

(m, 10 H, C–H aromatic), 8.22 (s, 1 H, N=C–H in the aminal), 8.31 (s, 2 H, N=C–H in the bisimine) ppm. $^{13}C\{^1H\}$ NMR (300 MHz, $CDCl_3$): δ = 44.99 (CH_2–N_{tert} in the aminal), 49.78 (CH_2–N_{sec} in the aminal), 53.38, 53.44 (CH_2–N– in the aminal and in the bisimine), 60.92, 61.09 (CH_2–N= in the aminal and in the bisimine), 83.59 (C–H in the aminal), 127.81, 128.08, 128.38, 128.55, 130.58, 136.07, 136.24, 140.62 (C aromatic), 161.73, 162.18 (N=C in the aminal and in the bisimine) ppm. FD-MS (CH_3CN): *m*/*z* (%) = 560 (43) $[2L^1]^+$, 280 (100) $[L^1]^+$. IR (KBr): $\tilde{\nu}$ = 3244 ν(N–H), 2925/2878/2839/2797 ν(C–H), 1645 ν(C=N), 758/696 δ(C–H).

***N*¹-Benzyl-*N*²-[2-(benzylamino)ethyl]ethane-1,2-diamine (L^2):** This preparation of the trihydrochloride salt of $\mathbf{L^2}$ has been described previously.[22] To a solution of $\mathbf{L^1}$ (4.00 g, 4.3 mmol) in absolute THF (100 mL) under N_2 was added $LiAlH_4$ (2.72 g, 71.0 mmol) in small portions with stirring before heating to reflux for 4 h. After cooling, H_2O (30 mL) was added cautiously to the suspension, which was stirred for a further 45 min at room temperature. The resulting white precipitate was collected by filtration and washed with THF (25 mL) and CH_2Cl_2 (25 mL). The filtrate was evaporated to dryness and the yellow residue was redissolved in CH_2Cl_2 (50 mL) and washed three times with NaOH (1 N, 25 mL). The organic phase was dried with Na_2SO_4 and evaporation of the solvent gave a yellow residue which was purified by kugelrohr distillation at 250 °C in vacuo to yield 2.88 g (10.4 mmol; 71%) of a yellow oil. FD-MS (CHI_3): *m*/*z* (%) = 283 (30) $[\mathbf{L^2}]^+$, 567 (100) $[2\,\mathbf{L^2}]^+$. IR (KBr): $\tilde{\nu}$ = 3303 ν(N–H), 3061/3027 ν(C–H aromatic), 2893/2818 ν(C–H aliphatic), 1453 δ(C–H aliphatic), 1115 ν(C–N), 738/700 δ(C–H aromatic). ^1H NMR ($CDCl_3$): δ = 1.60 (s, 3 H, NH), 2.71 (s, 8 H, CH_2), 3.77 (s, 4 H, CH_2–Ar), 7.22–7.30 (m, 10 H, H aromatic) ppm. $^{13}C\{^1H\}$ NMR ($CDCl_3$): δ = 48.87, 49.32 (CH_2), 53.93 (CH_2–Ar), 126.83, 128.07, 128.32, 140.49 (C aromatic) ppm. UV/Vis (CH_3CN): λ_{max} [nm] (ε [$M^{-1}cm^{-1}$]): 214 (19.062), 258 (shoulder, 1.142).

$[Cu(L^1)(CH_3CN)]PF_6$ (1): To a solution of $\mathbf{L^1}$ (0.419 g, 1.50 mmol) in MeOH (20 mL) was added $[Cu(CH_3CN)_4]PF_6$ (0.560 g, 1.50 mmol), which was stirred for 3 h at room temperature. The resulting yellow precipitate was collected by filtration, washed with diethyl ether and dried in vacuo to yield 0.289 g (0.59 mmol, 40%) of **1**. Yellow single crystals suitable for X-ray diffraction studies were obtained by diffusion of Et_2O into the a MeOH solution of **1**. $C_{20}H_{24}CuF_6N_4P$ (528.94): calcd. C 45.42, H 4.57, N 10.59; found C 45.49, H 4.85, N 10.53. ^1H NMR (300 MHz, [D_6]DMSO): δ = 2.08 (s, 3 H), 2.97 (m, 4 H), 3.77 (m, 4 H), 4.51 (s, 1 H), 7.36 (dd, 4 H), 7.56 (dd, 2 H), 8.09 (d, 4 H), 8.71 (s, 2 H) ppm. $^{13}C\{^1H\}$ NMR (300 MHz, [D_6]DMSO): δ = 0.00, 45.62, 59.37, 116.92, 127.27, 127.67, 131.04, 132.62, 163.92 ppm. FD-MS (MeH): *m*/*z* (%) = 622 (42) $[Cu(\mathbf{L^1})_2]^+$, 343 (100) $[Cu(\mathbf{L^1})]^+$, 281 (21) $[\mathbf{L^1}]^+$. IR (KBr): $\tilde{\nu}$ 3350 ν(N–H), 2962/2920/2868 ν(C–H), 1632 ν(C=N), 836 ν(P–F), 760/697 δ(C–H). UV/Vis (CH_3CN): λ_{max} [nm] (ε [$M^{-1}cm^{-1}$]) = 206 (52.381), 242 (29.766), 284 (4.584), 334 (3.119).

$[Cu_2(L^1)_2](ClO_4)_2$ (2): The dinuclear compound was synthesized in a similar manner to **1** in 80% yield. Red single crystals suitable for X-ray diffraction studies were obtained by diffusion of THF into the a MeOH solution of **2**. $C_{36}H_{42}Cl_2Cu_2N_6O_8$ (884.76): calcd. C 48.87, H 4.78, N 9.50; found C 48.85, H 4.85, N 9.33. ^1H NMR (300 MHz, [D_6]DMSO): δ = 2.98 (m, 8 H), 3.77 (m, 8 H), 4.51 (s, 2 H), 7.36 (dd, 8 H), 7.56 (dd, 4 H), 8.09 (d, 8 H), 8.71 (s, 4 H) ppm. $^{13}C\{^1H\}$ NMR (300 MHz, [D_6]DMSO): δ = 46.98, 66.73, 128.63, 129.03, 132.41, 133.98, 165.31 ppm. FD-MS (MeH): *m*/*z* (%) = 622 (11) $[Cu(\mathbf{L^1})_2]^+$, 442 (61) $[\{Cu(\mathbf{L^1})\}(ClO_4)]^+$, 343 (100) $[Cu(\mathbf{L^1})]^+$. IR (KBr): $\tilde{\nu}$ 3259 ν(N–H), 2909/2861 ν(C–H), 1627 ν(C=N), 1102 ν(Cl–O), 757/692 δ(C–H). UV/Vis (CH_3CN): λ_{max} [nm] (ε [$M^{-1}cm^{-1}$]) = 206 (99.393), 242 (60.722), 284 (8.853), 334 (5.902).

$[Cu_2(L^1)_2](BF_4)_2$ and $[Cu(L^1)(CH_3CN)]SbF_6$/$[Cu_2(L^1)_2](SbF_6)_2$: These compounds were synthesized analogously to **1** in 76% and 80% yield, respectively. Satisfactory ^1H, ^{13}C NMR and IR spectra and elemental analyses were obtained.

$[Cu(L^1)(PPh_3)](ClO_4)$ (3): To a suspension of $[Cu_2(\mathbf{L^1})_2](ClO_4)_2$ (0.442 g, 0.50 mmol) in MeOH (50 mL) was added PPh_3 (0.262 g, 1.00 mmol), which was stirred for 3 h at room temperature. The volume of the yellow solution was reduced to about 5 mL before the resulting yellow precipitate was collected by filtration, washed with diethyl ether and dried in vacuo to yield 0.58 g (0.82 mmol; 82%) of **3**. Yellow single crystals suitable for X-ray diffraction studies were obtained by diffusion of THF/Et_2O (1:1) into a CH_2Cl_2 solution of **3**. $C_{36}H_{36}ClCuN_3O_4P$ (704.67): calcd. C 61.37, H 5.14, N 5.96; found C 61.45, H 5.44, N 5.68. ^1H NMR (300 MHz, $CDCl_3$): δ = 2.92 (br. s, 2 H), 3.47 (br. s, 2 H), 3.59 [br. s, 1 H], 3.75 [br. s, 4 H], 6.83 (dd, 4 H), 7.11–7.37 (m, 17 H), 7.94 (d, 4 H), 8.61 (s, 2 H) ppm. $^{13}C\{^1H\}$ NMR (300 MHz, $CDCl_3$): δ = 48.28, 61.94, 128.63, 128.95 (d, ^3J = 9.45 Hz), 129.18, 130.15, 132.17, 132.18 (d, ^1J = 36.33 Hz), 133.13 (d, ^2J = 15.98 Hz), 133.27, 165.31 ppm. $^{31}P\{^1H, ^{13}C\}$ NMR (300 MHz, $CDCl_3$): δ = 2.38 (s) ppm. FD-MS ($CHCl_2$): *m*/*z* (%) = 604 (23) $[Cu(\mathbf{L^1})(PPh_3)]^+$, 441 (12) $[Cu(\mathbf{L^1})(ClO_4)]^+$, 342 (100) $[Cu(\mathbf{L^1})]^+$, 262 (9) $[PPh_3]^+$. IR (KBr): $\tilde{\nu}$ = 3317 ν(N–H), 3055 ν(C–H), 2918/2862 ν(C–H), 1632 ν(C=N), 1436 δ(C–H), 1092 ν(Cl–O), 751/696 δ(C–H). UV/Vis (CH_3CN): λ_{max} [nm] (ε [$M^{-1}cm^{-1}$]) = 210 (7.565), 236 (3.688), 278 (1.705), 362 (592).

$[Cu_2L^1_2(OCH_3)_2](PF_6)_2$ (4): To a solution of $\mathbf{L^1}$ (0.698 g, 2.50 mmol) in MeOH (20 mL) was added $[Cu(CH_3CN)_4]PF_6$ (0.933 g, 2.50 mmol), which was stirred under aerobic conditions for 3 h at room temperature. The resulting green precipitate was collected by filtration, washed with diethyl ether and dried in vacuo to yield 0.939 g (0.91 mmol, 73%) of **4**. Green single crystals suitable for X-ray diffraction studies were obtained by slow evaporation of the filtrate into the air. $C_{38}H_{48}Cu_2F_{12}N_6O_2P_2$ (1037.85): calcd. C 43.98, H 4.66, N 8.10; found C 44.11, H 5.03, N 7.81. FD-MS (MeH): *m*/*z* (%) = 342 (100) $[Cu(\mathbf{L^1})]^+$, 279/280 (10) $[\mathbf{L^1}]^+$. IR (KBr): $\tilde{\nu}$ = 3326 ν(N–H), 2929/2891/2820 ν(C–H), 1645 ν(C=N), 840 ν(P–F), 757/694 δ(C–H). UV/Vis (MeOH): λ_{max} [nm] (ε [$M^{-1}cm^{-1}$]) = 296 (8.185), 384 (734), 656 (238). μ_{eff} = 0 B.M.

$[Cu_2(L^1)_2(OH_2)](PF_6)_2$ (5): A solution of $[Cu(\mathbf{L^1})(CH_3CN)]PF_6$ (0.40 g, 0.757 mmol) in CH_2Cl_2 (15 mL) was cooled to –40 °C and bubbled with O_2 for 15 min. After stirring the suspension for 1.5 h at room temperature, the green precipitate was collected by filtration, washed with CH_2Cl_2 and dried at 100 °C in vacuo to yield 0.22 g (0.218 mmol; 58%) of **5**. Green single crystals suitable for X-ray diffraction studies were obtained by recrystallisation of the green precipitate from acetone at –20 °C. $C_{36}H_{44}Cu_2F_{12}N_6O_2P_2$ (1009.80): calcd. C 42.82, H 4.21, N 8.17; found C 42.84, H 4.42, N 8.50. FD-MS (MeH): *m*/*z* (%) = 343 (100) $[Cu(\mathbf{L^1})]^+$, 357 (10) $[Cu(\mathbf{L^1})O]^+$. IR (KBr): 3600 ν(O–H), 3330 ν(N–H), 3065 ν(C–H), 2941 ν(C–H), 1643 ν(C=N), 1453 ν (C–H), 842 ν(P–F), 758/694 δ(C–H). UV/Vis (MeCN): λ_{max} [nm] (ε [$M^{-1}cm^{-1}$]): 236 (11.874), 262 (11.526), 334 (2293), 626 (80). μ_{eff} = 0 B.M.

$[Cu_2(L^2)_2Cl_3]PF_6 \cdot 2MeOH$ (6): To a solution of $CuCl_2 \cdot 2H_2O$ (0.170 g, 1.00 mmol) and NH_4PF_6 (0.082 g, 0.50 mmol) in CH_3CN (20 mL) was added $\mathbf{L^2}$ (0.283 g, 1.00 mmol) in MeOH (10 mL). The mixture was stirred for 30 min at room temperature. The resulting blue precipitate was collected by filtration and recrystallised from a mixture of $CHCl_3$ and MeOH to yield 0.160 g (0.162 mmol; 32%) of **6** as crystals, which were suitable for X-ray diffraction. $C_{36}H_{50}Cl_3Cu_2F_6N_6P$ (M = 977.21 g/mol): calcd. C 45.75, H 5.33, H 8.89; found C 45.80, H 6.07, N 9.01. FD-MS (CH_3CN): *m*/*z* (%)

= 799 (53) $[Cu_2(\mathbf{L^2})_2Cl_3]^+$, 381 (100) $[Cu(\mathbf{L^2})Cl]^+$, 284 (43) $[\mathbf{L^2}]^{+\cdot}$. IR (KBr): $\tilde{\nu}$ = 3278/3256/3183 ν(N–H), 2953/2890 ν(C–H aliphatic), 1454 δ(C–H aliphatic), 840 ν(P–F), 751/703 ν(C–H aromatic). UV/Vis (MeOH, λ_{max} [nm] (ε [$M^{-1}cm^{-1}$])): 298 (9.537), 660 (173). μ_{eff} (298 K) = 1.82 B.M.

Investigation of the Potential Hydroxylation Reaction of the Ligand: A solution of $[Cu(\mathbf{L^1})(CH_3CN)]PF_6$ (0.793 g, 1.50 mmol) in CH_2Cl_2 (20 mL) was bubbled with O_2 at –40 °C for 20 min and warmed to room temperature. After stirring the green suspension for 1.5 h, it was extracted five times into of a 2:1 mixture of NH_3 (25%) and brine (30 mL). The combined aqueous phases were then washed with CH_2Cl_2 (50 mL). The combined organic phases were dried with Na_2SO_4 and the solvents evaporated to dryness. The resulting brown oil was dried in vacuo to yield 65% of a mixture of $\mathbf{L^1}$ and the decomposition product benzaldehyde. This was ascertained by ^1H and ^{13}C NMR spectroscopy and mass spectrometry. In the IR spectrum, no absorption band for a potential O–H vibration was observed.

Quantitative Investigation of H_2O_2 Formation upon Oxidation: A solution of $\mathbf{L^1}$ (0.559 g, 2.00 mmol) and $[Cu(CH_3CN)_4]PF_6$ (0.745 g, 2.00 mmol) in CH_2Cl_2 (50 mL) was bubbled with O_2 for 5 min at –40 °C. The resulting green solution was warmed to –30 °C and the reaction was quenched with HPF_6 (4.84 g, 20.00 mmol, 60%) in Et_2O (10 mL). After warming to room temperature, the suspension was stirred for 10 min. The brown precipitate was collected by filtration and talen up in Et_2O (10 mL). To this solution was added a solution of KI (1.0 g) in H_2O (25 mL) and concentrated acetic acid (10 mL). After stirring the solution for 20 min it was titrated with $Na_2S_2O_3$ solution (0.1 N) using a freshly prepared starch solution as indicator to yield on average 7.8% H_2O_2 (referring to 100% formation of the peroxido species).

Selected bond lengths [Å] and angles [°] for **1** to **5** are given in Tables 1, 2, 3, 4 and 5.

CCDC-720275 (for $\mathbf{L^1}$), -163359 (for **1**), -720276 (for **2**), -720277 (for **3**), -720278 (for **4**), -720279 (for **5**), contain the supplementary crystallographic data for this paper. These data can be obtained free of charge from The Cambridge Crystallographic Data Centre via www.ccdc.cam.ac.uk/data_request/cif.

Supporting Information (see also the footnote on the first page of this article): Detailed crystallographic data of $\mathbf{L^1}$ and complexes **1**–**5**.

Acknowledgments

The authors gratefully acknowledge financial support from the Deutsche Forschungsgemeinschaft (DFG). Furthermore, they thank Prof. Rudi van Eldik (University of Erlangen-Nürnberg) for supporting this work. Diana Utz is thankful for a scholarship from the University of Erlangen-Nürnberg. Dr. Achim Zahl (University of Erlangen-Nürnberg) is acknowledged for his assistance with the NMR measurements.

[1] a) S. R. Collinson, D. E. Fenton, *Coord. Chem. Rev.* **1996**, *148*, 19–40; b) S. M. Nelson, *Pure Appl. Chem.* **1980**, *52*, 461–2476.

[2] a) K. D. Karlin, Z. Tyeklár (Ed.), *Bioinorganic Chemistry of Copper*, Chapman & Hall, Inc., New York, London, **1993**; b) E. I. Solomon, P. Chen, M. Metz, S.-K. Lee, A. E. Palmer, *Angew. Chem. Int. Ed.* **2001**, *40*, 4570–4590; c) H. Decker, T. Schweikardt, F. Tuczek, *Angew. Chem. Int. Ed.* **2006**, *45*, 4546–4550; d) H. Decker, R. Dillinger, F. Tuczek, *Angew. Chem. Int. Ed.* **2000**, *39*, 1591–1595; e) A. Sánchez-Ferrer, J. N. Rodriguéz-López, F. García-Cánovas, F. García-Carmona, *Biochim. Biophys. Acta* **1995**, *1247*, 1–11; f) J. C. Garcia-Borron, F. Solano, *Pigment Cell Res.* **2002**, *15*, 162–173; g) C. M. Marusek, N. M. Trobaugh, W. H. Flurkey, J. K. Inlow, *J. Inorg. Biochemistry* **2006**, *100*, 108–123; h) N. Wang, D. N. Hebert, *Pigm. Cell Res.* **2006**, *19*, 3–18; i) E. I. Solomon, U. M. Sundaram, T. E. Machonkin, *Chem. Rev.* **1996**, *96*, 2563–2606; j) H. Claus, H. Decker, *Syst. Appl. Microbiol.* **2006**, *29*, 3–14; k) Y. Matoba, T. Kumagai, A. Yamamoto, H. Yoshitsu, M. Sugiyama, *J. Biol. Chem.* **2006**, *281*, 8981–8990.

[3] a) L. Casella, M. Gulotti, G. Pallanza, L. Rigoni, *J. Am. Chem. Soc.* **1988**, *110*, 4221–4227; b) L. Casella, M. Gulotti, M. Partosek, G. Pallanza, E. Lauretini, *J. Chem. Soc., Chem. Commun.* **1991**, 1235–1237; c) O. J. Gelling, A. Meetsma, F. v. Bolhuis, B. L. Feringa, *J. Chem. Soc., Chem. Commun.* **1988**, 552–554; d) D. Gosh, R. Mukherjee, *Inorg. Chem.* **1998**, *37*, 6597–6605; e) K. D. Karlin, J. C. Hayes, Y. Gultneh, R. W. Cruse, J. W. McKnown, J. P. Hutchinson, J. Zubieta, *J. Am. Chem. Soc.* **1984**, *106*, 2121–2139; f) S. Mandal, R. Mukherjee, *Inorg. Chim. Acta* **2006**, *359*, 4019–4026; g) S. Palavicini, A. Granata, E. Monzani, L. Casella, *J. Am. Chem. Soc.* **2005**, *127*, 18031–18036; h) L. Li, A. N. Sarjeant, K. D. Karlin, *Inorg. Chem.* **2006**, *45*, 7160–7172; i) E. A. Lewis, W. B. Tolman, *Chem. Rev.* **2004**, *104*, 1047; j) M. S. Nasir, K. D. Karlin, D. McGowty, J. Zubieta, *J. Am. Chem. Soc.* **1991**, *113*, 698–701; k) R. W. Cruse, S. Kaderli, K. D. Karlin, A. D. Zuberbühler, *J. Am. Chem. Soc.* **1988**, *110*, 6882–6883; l) M. Becker, S. Schindler, K. D. Karlin, T. A. Kaden, S. Kaderli, T. Palanche, A. D. Zuberbühler, *Inorg. Chem.* **1999**, *38*, 1989–1995; m) K. D. Karlin, M. S. Nasir, B. I. Cohen, R. W. Cruse, S. Kaderli, A. D. Zuberbühler, *J. Am. Chem. Soc.* **1994**, *116*, 1324–1336; n) G. Battaini, L. Casella, M. Gullotti, E. Monzani, G. Nardin, A. Perotti, L. Randaccio, L. Santagostini, F. W. Heinemann, S. Schindler, *Eur. J. Inorg. Chem.* **2003**, 1197–1205; o) O. Sander, A. Henß, C. Näther, C. Würtele, M. C. Holthausen, S. Schindler, F. Tuczek, *Chem. Eur. J.* **2008**, *14*, 9714–9729.

[4] a) R. Menif, A. E. Martell, *J. Chem. Soc., Chem. Commun.* **1989**, 1521–1523; b) R. Menif, A. E. Martell, P. J. Squattrito, A. Clearfield, *Inorg. Chem.* **1990**, *29*, 4723–4729; c) D. Utz, F. W. Heinemann, F. Hampel, D. T. Richens, S. Schindler, *Inorg. Chem.* **2003**, *42*, 1430–1436; d) M. Becker, S. Schindler, R. v. Eldik, *Inorg. Chem.* **1994**, *33*, 5370–5371; e) H. Ma, M. Allmendinger, U. Thewalt, A. Lentz, M. Klinga, B. Rieger, *Eur. J. Inorg. Chem.* **2002**, 2857–2867.

[5] a) A. Company, L. Gómez, R. n. Mas-Balleste, I. V. Korendovych, X. Ribas, A. Poater, T. Parella, X. Fontrodona, J. Benet-Buchholz, M. Sola, J. L. Que, E. V. Rybak-Akimova, M. Costas, *Inorg. Chem.* **2007**, *46*, 4997–5012; b) A. Llobet, A. E. Martell, M. A. Martínez, *J. Mol. Catal. A* **1998**, *129*, 19–26.

[6] A. Poater, *J. Phys. Chem. A* **2009**, *113*, 9030–9040.

[7] H. Adams, N. A. Bailey, D. E. Fenton, P. D. Hempstead, G. P. Westwood, *J. Incl. Phenom. Mol. Recognit. Chem.* **1991**, *11*, 63–69.

[8] a) P. Comba, A. Fath, T. W. Hambley, D. T. Reichens, *Angew. Chem. Int. Ed. Engl.* **1995**, *34*, 1883–1884; b) L. J. Childs, N. W. Alock, M. J. Hannon, *Angew. Chem. Int. Ed.* **2001**, *40*, 1079–1080; c) M. Wenzel, S. R. Bruere, Q. W. Knapp, P. A. Tasker, P. G. Plieger, *Dalton Trans.* **2010**, *39*, 2936–2941.

[9] N. K. Solanki, A. E. H. Wheatley, S. Radojevic, M. McPartlin, M. A. Halcrow, *J. Chem. Soc., Dalton Trans.* **1999**, 521–523.

[10] a) C. V. K. Sharma, S. T. Griffin, R. D. Rogers, *Chem. Commun.* **1998**, 215–216; b) M. A. Withersby, A. J. Blake, N. R. Champness, P. Hubberstey, W. S. Li, M. Schroder, *Angew. Chem. Int. Ed. Engl.* **1997**, *36*, 2327–2329; c) L. R. Hanton, K. Lee, *J. Chem. Soc., Dalton Trans.* **2000**, 1161–1166.

[11] B. Hasenkopf, J.-M. Lehn, N. Boumediene, A. Dupont-Gervais, A. v. Dorsselaer, B. Kneisel, D. Fenske, *J. Am. Chem. Soc.* **1997**, *119*, 10956–10962.

[12] M. J. Hannon, C. L. Painting, E. A. Plummer, L. J. Childs, N. W. Alcock, *Chem. Eur. J.* **2002**, *8*, 2225–2238.

[13] W. Schiessl, R. Puchta, Z. D. Bugarcic, F. W. Heinemann, R. v. Eldik, *Eur. J. Inorg. Chem.* **2007**, 1390–1404.
[14] K. T. Pots, M. Keshavarz-K, F. S. Tham, H. D. Abruna, C. Arana, *Inorg. Chem.* **1993**, *32*, 4450–4456.
[15] A. W. Addison, T. N. Rao, J. Reedijk, J. v. Rijn, G. C. Verschoor, *J. Chem. Soc., Dalton Trans.* **1984**, 1349–1356.
[16] H. Ma, M. Allmmendinger, U. Thewalt, A. Lentz, M. Klinga, B. Rieger, *Eur. J. Inorg. Chem.* **2002**, 2857–2867.
[17] a) M. Weitzer, M. Schatz, F. Hampel, F. W. Heinemann, S. Schindler, *J. Chem. Soc., Dalton Trans.* **2002**, 686–694; b) M. Becker, F. W. Heinemann, S. Schindler, *Chem. Eur. J.* **1999**, *5*, 3124–3129; c) C. X. Zhang, S. Kaderli, M. Costas, E.-i. Kim, Y.-M. Neuhold, K. D. Karlin, A. D. Zuberbühler, *Inorg. Chem.* **2003**, *42*, 1807–1824; d) M. Weitzer, S. Schindler, G. Brehm, S. Schneider, E. Hörmann, B. Jung, S. Kaderli, A. D. Zuberbühler, *Inorg. Chem.* **2003**, *42*, 1800–1806.
[18] a) R. A. Himes, K. D. Karlin, *Proc. Natl. Acad. Sci. USA* **2009**, *106*, 18877–18878; b) J. S. Woertinka, P. J. Smeetsa, M. H. Groothaert, M. A. Vancea, B. F. Selsb, R. A. Schoonheydt, E. I. Solomon, *Proc. Natl. Acad. Sci. USA* **2009**, *106*, 18908–18913; c) R. Balasubramanian, S. M. Smith, S. Rawat, L. A. Yatsunyk, T. L. Stemmler, A. C. Rosenzweig, *Nature* **2010**, *465*, 115–U131.
[19] K. D. Karlin, Y. Gulthneh, J. C. Hayes, J. Zubieta, *Inorg. Chem.* **1984**, *23*, 519–521.
[20] a) M. Taki, S. Teramae, S. Nagamoto, Y. Tachi, T. Kitagawa, S. Itoh, S. Fukuzumi, *J. Am. Chem. Soc.* **2002**, *124*, 6367–6377; b) P. L. Holland, K. R. Rodgers, W. B. Tolman, *Angew. Chem. Int. Ed.* **1999**, *38*, 1139–1142; c) S. Itoh, S. Fukuzumi, *Bull. Chem. Soc. Jpn.* **2002**, *75*, 2081–2095.
[21] S. Ryan, H. Adams, D. E. Fenton, M. Becker, S. Schindler, *Inorg. Chem.* **1998**, *37*, 2134–2140.
[22] J. A. Scafani, M. T. Maranto, T. M. Sisk, S. A. v. Armin, *J. Org. Chem.* **1996**, *61*, 3221–3222.
[23] a) M. Schatz, M. Becker, O. Walter, G. Liehr, S. Schindler, *Inorg. Chim. Acta* **2001**, *324*, 173–179; b) J. Astner, M. Weitzer, S. P. Foxon, S. Schindler, F. W. Heinemann, J. Mukherjee, R. Gupta, V. Mahadevan, R. Mukherjee, *Inorg. Chim. Acta* **2007**, *361*, 279–292.
[24] a) R. D. Köhn, G. Seifert, G. Kociok-Köhn, *Chem. Ber.* **1996**, *129*, 1327–1333; b) P. Gentschev, A. A. Feldmann, M. Lüken, N. Möller, H. Sirges, B. Krebs, *Inorg. Chem. Commun.* **2002**, *5*, 64–66; c) K. D. Karlin, J. W. McKnown, J. C. Hayes, J. P. Hutchinson, J. Zubieta, *Transition Met. Chem.* **1984**, *9*, 405–406; d) Y. Kani, S. Ohba, S. Ito, Y. Nishida, *Acta Crystallogr., Sect. C: Cryst. Struct. Commun.* **2000**, *56*, e195–e195.
[25] G. J. Kubas, *Inorg. Synth.* **1979**, *19*, 90–92.
[26] M. Weitzer, M. Schatz, F. Hampel, F. W. Heinemann, S. Schindler, *J. Chem. Soc., Dalton Trans.* **2002**, 686–694.
[27] S. V. Kryatov, E. V. Rybak-Akimova, S. Schindler, *Chem. Rev.* **2005**, *105*, 2175–2226.
[28] G. M. Sheldrick, in: *SHELXTL NT*, Bruker Analytical Instruments, Madison, WI, **1998**.
[29] R. H. Blessing, *Acta Crystallogr., Sect. A* **1995**, *51*, 33–3.

Received: September 8, 2010
Published Online: November 25, 2010

